Large-scale molecular dynamics simulations of shock induced plasticity in tantalum single crystals

R. Ravelo, Qi An, Timothy C. Germann, and B.L. Holian

Citation: AIP Conference Proceedings **1426**, 1263 (2012); doi: 10.1063/1.3686510
View online: http://dx.doi.org/10.1063/1.3686510
View Table of Contents: http://scitation.aip.org/content/aip/proceeding/aipcp/1426?ver=pdfcov
Published by the AIP Publishing

LARGE-SCALE MOLECULAR DYNAMICS SIMULATIONS OF SHOCK INDUCED PLASTICITY IN TANTALUM SINGLE CRYSTALS

Ramon Ravelo[1, 2], **Qi An**[3], **Timothy C. Germann**[2] **and Brad Lee Holian**[2]

[1] *Physics Department and Materials Research Institute, University of Texas, El Paso, TX 79968*
[2]*Los Alamos National Laboratory, Los Alamos, NM 87545*
[3]*Materials and Process Simulation Center, California Institute of Technology, Pasadena CA 91125*

Abstract. We report on large-scale non-equilibrium molecular dynamics (NEMD) simulations of shock wave compression in Ta single crystals. The atomic interactions are modeled via a recently developed and optimized embedded-atom method (EAM) potential for Ta, which reproduces the equation of state up to 200 GPa. We examined the elastic-plastic transition and shock wave structure for wave propagation along the low index directions: (100), (110) and (111). Shock waves along (100) and (111) exhibit an elastic precursor followed by a plastic wave for particle velocities below 1.1 km/s for (100) and 1.4 km/s for (111). The nature of the plastic deformation along (110) is dominated by twinning for pressures above 41 GPa.

Keywords: Shock waves, molecular dynamics, metals, bcc, twinning, plasticity.
PACS: 62.50.Ef, 64.30.Ef, 61.72.Mm.

INTRODUCTION

Tantalum is a bcc transition metal whose simple phase diagram exhibits no known solid-solid phase changes with pressure or temperature. Due to its high melting temperature and strength, it is widely used in the production of high-temperature superalloys for many technological applications. Recently, there has been an increased interest in the mechanical and strength properties of Ta at high pressures and high deformation strains and strain-rates. While there have been many computational studies of thermal and mechanical properties of Ta at high pressures [1], [2], there has been, to date, no systematic simulation study of the dynamical response of Ta to shock wave and high strain rate loading. We have carried out large-scale non-equilibrium molecular dynamics (NEMD) simulations of shock-wave propagation in Ta single crystals along the low-index directions (100), (110), and (111). The atomic interactions were modeled by a newly developed embedded atom method (EAM [3]) interatomic potential. Plastic deformation mechanisms, anisotropic shock wave structure, and Hugoniot elastic limits were examined as functions of crystal orientation for pressures up to 200 GPa.

METHODOLOGY

Several semi-empirical interatomic models of Ta have been developed over the years. These include models based on EAM [4], [5] as well as the Finnis-Sinclair (FS) parameterization scheme [6]-[9]. Except for Refs. [7] and [9], these potential models were not specifically developed for high pressure-high temperature applications. As a result, high-pressure properties are reproduced with various degrees of success. Since Ta has no known solid-solid phase changes with pressure, one criterion we employed to test the transferability of several interatomic potential models was the stability

Shock Compression of Condensed Matter - 2011
AIP Conf. Proc. 1426, 1263-1266 (2012); doi: 10.1063/1.3686510

of the bcc phase with respect to other energetically close phases. For EAM potentials, one such measure is the bcc-hcp enthalpy difference as a function of pressure. All models tested using this criterion exhibit a bcc→hcp transition in the range 35-85 GPa (Fig 1).

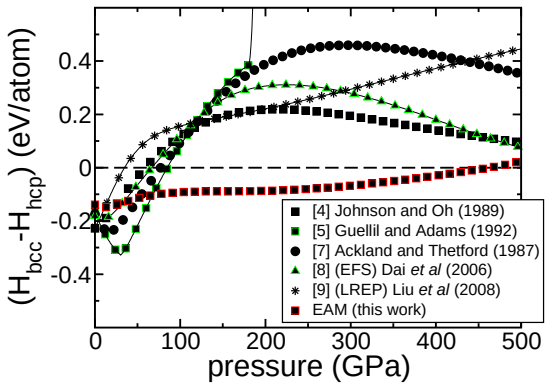

Figure 1. Enthalpy difference (bcc-hcp) as a function of pressure ($T = 0$) from various semi-empirical interatomic potential models of Ta and the EAM model of this work.

We developed a new EAM interatomic potential of Ta with the goal of extending the range of transferability of the model with no solid-solid phase transitions within 0-460 GPa ($T = 0$). The fitting database included both experimental and density functional theory (DFT) data: lattice constant, cohesive energy, unrelaxed vacancy formation energy, elastic constants, equation of state (EOS) of various phases: bcc, fcc, hcp and A15. Details on the functional forms and quantitative comparisons with experimental and DFT data will be provided in a forthcoming publication [10].

Shock compression was studied via large-scale (multi-million atom) non-equilibrium molecular dynamics (NEMD) simulations. The procedure we employed to initiate a shock wave of a given strength is detailed in Ref. [11]: the crystal impacts an infinitely massive piston with a velocity u_p. The velocity of the slab against the piston was ramped linearly from 0 to u_p in 5-10 ps, in order to minimize heating near the impact surface. The impact produces a shock wave that propagates away from the piston at shock velocity u_s. The targets consisted of Ta rectangular slabs with cross sections of (20 nm × 20 nm) and (66 nm × 66 nm) and up to 500 nm long. Periodic boundary conditions were imposed in the transverse (x- and y-) directions and free boundaries in the longitudinal direction (shock direction). The initial temperature of the Ta sample was set to 300 K.

We also carried out constant-stress Hugoniostat simulations in order to probe longer time scales (~100 ps) and sample more points along the Hugoniot. Details of the method can be found in [12]. The simulation samples were comprised of up to 100,000 particles in a cube. The uniaxial compression was applied along the low-index crystallographic directions (100), (110), and (111), and the strain-rate was selected to approximate the rise times of the shock profiles in the NEMD simulations.

RESULTS AND DISCUSSION

Figure 2 shows the u_s-u_p Hugoniot of Ta for shocks along (100), (111), and (110). Also shown is a fit to experimental data from Refs. [13] and [14], extrapolated to zero pressure. All three directions exhibit a split-wave regime, with shocks along (111) exhibiting the highest longitudinal stress at the overdriven point and (110) having the lowest (115 GPa and 47 GPa, respectively).

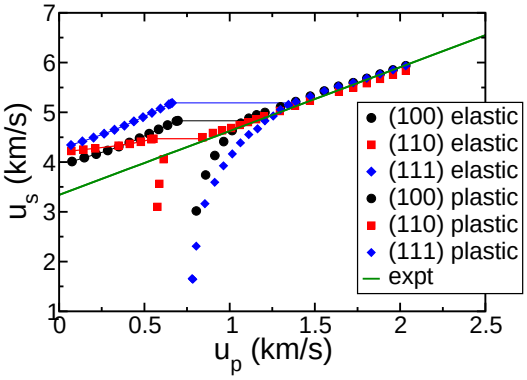

Figure 2. Shock Hugoniot of Ta single crystals for wave propagation along (100), (110), and (111) crystallographic directions. The experimental line is a fit to shock data from Refs. [13] and [14].

Shock profiles along (100) and (111) directions are characterized by a solitary wave train ahead of the elastic precursor for particle velocities below the overdriven (OD) point. This can be seen in Fig. 3, which shows typical stress and atomic configuration profiles in the split-wave regime for shocks along (100) and (111). The critical shear

stress at the Hugoniot elastic limit (τ_{HEL}) can be inferred from the shear stress profile of the elastic precursor and more accurately from Hugoniostat simulations. The values of τ_{HEL} for (110), (100), and (111) are 5.0, 12.5, and 14.5 GPa, respectively.

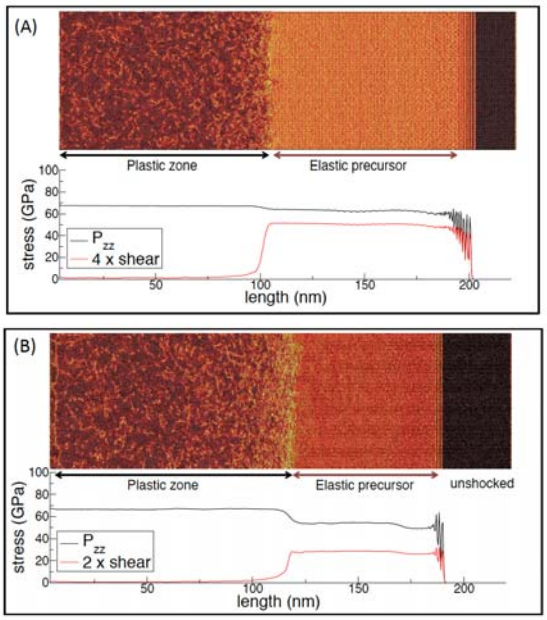

Figure 3. Atomic configuration and stress profiles of (A) Ta(100) (u_p=0.88 km/s) and (B) Ta(111) (u_p=0.88 km/s). Atoms are colored according to local strain.

Shock-induced twinning in Ta

The primary plastic deformation mechanism for shock wave propagation along (110) is clearly different than for (100) and (111) shocks. Deformation twinning is the main stress relaxation mechanism in shock wave propagation along (110) for values of u_p between 0.60 and 1.00 km/s (40-90 GPa). Twins nucleate at the shock front, quickly grow, and thicken behind the shock (see Fig. 4). The thickening of the twins is accompanied by dislocation nucleation and multiplication, consistent with inelastic strain buildup produced or accompanied by thickening of the twins. This can be seen in greater detail in Fig 5, which shows a time sequence of twin nucleation in a 40x40x40 nm^3 sample homogeneously compressed along (110) 13.5% (~45 GPa). The bottom sequence shows atoms colored according to the orientation-imaging map (OIM): green regions have (110) planes oriented along compression direction (*Z*); twin bands are identified in red. In the top sequence, which shows only defect atoms, dislocations nucleate between twins on a longer time scale.

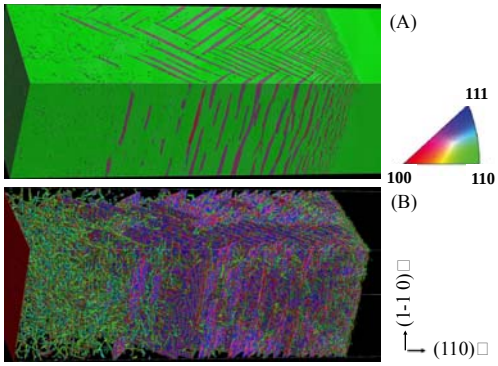

Figure 4. Detail twin formation pattern in Ta single crystals shocked along (110) (u_p=0.62 km/s, P_{zz}=42 GPa). (A) Orientation imaging map (OIM). (B) Defect structure associated with (A). Only defect atoms are shown.

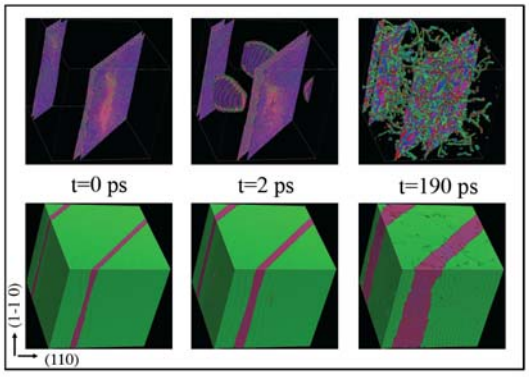

Figure 5. Time snapshots of twin nucleation in Ta compressed homogeneously along (110) by 13.5%. The top sequence shows defective atoms while the bottom shows atoms colored according to the OIM map as in Fig. 4.

The fact that deformation twinning is observed in (110) at lower stress levels than in (100) and (111) [the shear stress at the HEL in the (110) direction is the lowest of the three] indicates that this is the easiest direction for deformation twinning, perhaps due to a preferred orientation between parent and twin lattices. However, once they are nucleated, dislocations nucleate between the twins, further reducing the shear stress. Twin bands continually anneal out behind the shock front in those

regions where the shear stress drops below 1-1.5 GPa.

At higher shock compressions and corresponding higher stress levels, deformation twinning competes less with dislocation nucleation. For particle velocities above 1.2 km/s, twins are no longer nucleated at the shock front (Fig. 6).

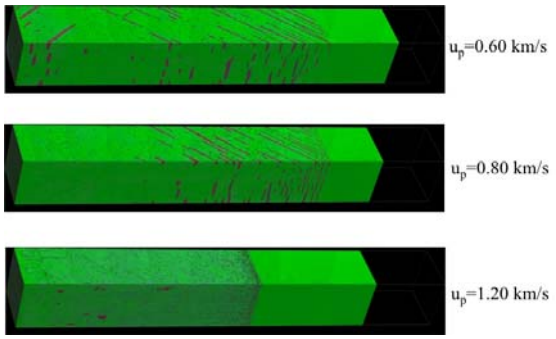

Figure 6. Defect structures in Ta single crystal shocked along (110). Atoms are colored according to OIM. Twin formation is clearly visible for u_p=0.60 and 0.80 km/s. Above 1.2 km/s deformation twinning is no longer the main mechanism of stress relation.

CONCLUSIONS

We have carried out large-scale NEMD and Hugoniostat simulations of shock wave compression of Ta single crystals, examining the nature of the plastic deformation and elastic limits as functions of crystal orientation. All directions studied [(100), (110), and (111)] exhibit two-wave structures for particle velocities between 0.6 km/s and 1.0 km/s. Shocks along (100) and (111) exhibit a solitary wave train ahead of the elastic precursor. The plastic deformation in these two directions is characterized by dislocation nucleation and multiplication, with densities that increase with pressure to values of 10^{13} cm^{-2} at pressures of 80-90 GPa. In contrast, plastic deformation in shock compression along (110) is due primarily to the formation of twins that nucleate at the shock front. However, for particle velocities above 1.2 km/s (~90 GPa), twinning no longer is the main precursor to plastic deformation. Above this pressure, the defect structures and densities along (110) are very nearly the same as to those found in (100) and (111) shocks at corresponding pressures.

ACKNOWLEDGEMENTS

Part of this work was supported by the U.S. Department of Energy under contract DE-AC52-06NA25396. The authors thank James E. Hammerberg, Davis Tonks and Sheng-Nian Luo for useful discussions and valuable comments.

REFERENCES

1. Moriarty, J. A., et al., J. Phys. Condens. Matter **14**, 2825 (2002).
2. Orlikowski, D., Söderlind, P., and Moriarty, J. A., Phys. Rev. B **74**, 054109 (2006).
3. Daw, M. S., Baskes, M. I., Phys. Rev. B **29**, 6443 (1984).
4. Johnson, R. A., and Oh, D. J., J. Mater. Res. **4**, 1195 (1989).
5. Guellil, A. M., and Adams, J. B., J. Mater. Res. **7**,639 (1992).
6. Finnis, M. W., and Sinclair J. E., Phil. Mag. A **50**, 45 (1984).
7. Ackland, G. J,. and Thetford, R., Phil. Mag. A **56**, 15 (1987).
8. Dai, X. D., Kong, Y., Li, J. H., and Liu, B. X., J. Phys. Condens. Matter **18**, 4527 (2006).
9. Liu, Z. L., Cai, L. C., Chen, X. R., and Jing, F. Q., Phys. Rev. B **77**, 024103 (2008).
10. Ravelo, R., et al. (to be submitted).
11. Holian B. L., and Lomdahl P. S., Science **80**, 2085 (1998).
12. Ravelo, R., Holian, B. L., Germann, T. C., and Lomdahl P. S., Phys. Rev. B **70**, 014103 (2004).
13. Marsh, S.P. *LASL Shock Hugoniot Data*, University of California Press, Los Alamos (1980).
14. Mitchell, A. C., and Nellis, W. J., J. Appl. Phys. **52**, 3363 (1981).